# Investigating Computational Challenges in Mixed-Fleet EVRP with Lunch and Charging Constraints

NETIPHAN AMPHAIPHAN [1], DARIO LANDA-SILVA [2], WASAKORN LAESANKLANG [1,3]
[1]Department of Mathematics, Faculty of Science, Mahidol University, Bangkok
THAILAND

[2]School of Computer Science, University of Nottingham, Nottingham
UNITED KINGDOM

[3]Centre of Excellence in Mathematics, MHESI, Bangkok
THAILAND

*Abstract:* Using a mixed fleet of internal combustion and electric vehicles in logistics ensures operational reliability while gradually reducing emissions and adapting to evolving infrastructure. This study extends the Electric Vehicle Routing Problem (EVRP) to include mixed fleets, partial recharging, diverse charging technologies, and mandatory driver lunch breaks in urban logistics. A mixed-integer programming (MIP) model minimizes total operational costs, including travel distance, vehicle use, charging, and non-productive time. Using real delivery data from a Bangkok logistics provider, 34 problem instances were generated. Results show that only six small instances solved optimally within 15 minutes. Incorporating lunch break constraints does not significantly increase operating costs or fleet utilization. To address scalability, a hybrid approach combining K-means clustering with exact optimization was developed, yielding feasible solutions for all instances and faster computation. In several cases, clustering preserved or improved solution quality when aligned with customer geography.

*Key-Words:* Mixed fleet electric vehicle, vehicle routing problem, location and routing, mixed integer programming, clustering, driver lunch break.

Received: September 16, 2026. Revised: October 7, 2026. Accepted: October 21, 2026. Published: November 26, 2026.

## 1 Introduction

### 1.1 Background and motivation

Climate change and environmental pollution are pushing industries to cut greenhouse gas emissions and particulate matter (PM). Logistics is one of the largest global energy consumers and relies heavily on fossil fuels. The Sustainable Development Goals (SDGs) call on the sector to reduce energy use and emissions through better vehicle efficiency and more renewable energy in the fuel mix. Pathways to more sustainable logistics include reducing transport demand, eliminating unnecessary trips, switching to low-emission fuels, and improving vehicle efficiency. Recent geopolitical shocks reinforce this urgency. The 2026 US–Iran conflict disrupted shipping through the Strait of Hormuz and triggered one of the largest oil-supply shocks on record. Brent crude surged more than 50% within a single month, exposing the vulnerability of fossil-fuel logistics to supply and price risk [1]. Such episodes strengthen the case for electrifying logistics fleets. Electric vehicles (EVs) offer a more energy-efficient and low-emission alternative to internal combustion engine vehicles [2]. They also cost less to operate: maintenance requirements are lower, and electricity is generally cheaper than fossil fuels.

EVs also face limitations. Battery capacity is restricted, charging stations (CSs) are not yet widely available, and charging takes time. As a result, logistics companies have gradually integrated EVs into their fleets alongside ICVs. This adds complexity to route planning: operators must decide when vehicles recharge and schedule visits to CSs.

Logistics companies typically rely on classical vehicle routing problems (VRPs) to plan their delivery routes. VRPs seek to minimize total operational costs when serving a set of customers while satisfying constraints such as time windows, customer demands, and vehicle capacity. Over the years, VRPs have been extended in numerous ways to address real-world operational challenges. The Electric Vehicle Routing Problem (EVRP) is one of those extensions [2], [3], [4], [5]. EVRP considers a set of vehicles along with a set of charging stations. Vehicle routes may need to include visits to charging stations to ensure that the journey can be completed and the vehicle can return to the depot without depleting its battery.

To reflect real-world operating conditions, it is important to incorporate mandatory driver lunch breaks into the routing model. This constraint has been considered in prior studies across various application domains, including waste collection [6], pet food delivery [7], and furniture delivery [8]. The lunch break constraint requires drivers to pause at an intermediate location along their route, ensuring compliance with labor regulations and company policy. Incorporating this constraint into the EVRP presents an additional opportunity: EVs can be recharged during the break, thereby combining rest time with productive charging. Nevertheless, studies

that jointly consider a mixed fleet (comprising both EVs and ICVs) and driver lunch breaks remain scarce in the literature.

As technology advances, this paper proposes a method for creating a vehicle routing plan suited to courier firms operating a mixed fleet of conventional and electric vehicles (EVs), while also accommodating driver lunch breaks. The challenge is formulated as a mixed integer programming (MIP) model. The task is for a set of vehicles to meet customer demands within specified time windows. Given the limited range of EVs, charging stations are essential for replenishing energy to complete routes. There are two distinct charging technologies available, 20 and 45 kilowatts (kW). Each offers different charging times and costs. It is assumed that EVs are compatible with both technologies and can visit charging station no more than once in a day. Furthermore, to preserve battery longevity, it is recommended that EVs be charged within the 25%-80% state-of-charge range [8], [9], [10], an operational constraint incorporated into our model. Hence, permitting partial recharges at stations not only reduces costs and charging time but also prolongs battery life. Additionally, synchronizing vehicle recharging with driver lunch breaks could offer further benefits.

## 1.2 Literature Review

In this subsection, we review studies related to EVRP and its variants, covering mixed-fleet configurations, partial recharging strategies, diverse charging technologies, and driver lunch break constraints. For a broader overview of EVRP variants and solution approaches, readers are referred to the comprehensive surveys by [11], [12].

[13] introduced the Green Vehicle Routing Problem (G-VRP), which considers Alternative Fuel Vehicles (AFVs) with limited driving range. Due to their limited driving range, these vehicles may need to stop at refueling stations during their routes. Later, [5] examined the Electric Vehicle Routing Problem with time windows and recharging stations. Given the limited energy capacity of these vehicles, planned routes require visits to recharging stations. Notably, the duration of charging at these stations depends significantly on the vehicle's remaining battery level.

Early EVRP studies generally assumed that EVs must be recharged to their maximum battery level. However, [3], [14], [15], [16] introduced a more flexible approach by allowing partial recharges, effectively reducing charging time. Furthermore, [3] also considered the impact of different charging technologies on the charging time.

[17] contributed a novel perspective to EVRP by studying the effect of load on energy consumption, focusing on mixed services for customers involving both delivery and pickup, while disregarding customers' time windows. [18] investigated a mixed fleet VRP consisting of EVs and ICVs, noting the variations in battery capacities and operating costs among EVs. They also highlighted that not all EVs are compatible with the multiple charging technologies available at charging stations.

Additionally, [19], [20] examined a mixed fleet VRP. The latter study incorporated a realistic energy consumption model dependent on factors such as speed, gradient, and cargo load distribution. [21] further expanded on this concept by studying a mixed fleet VRP with partial recharges and applying realistic energy functions to both EVs and ICVs.

[22], [23] studied a mixed fleet comprising EVs and ICVs with the aim to reduce greenhouse gas emissions. Greenhouse gas emission constraints applicable to ICVs were proposed by [24]. Similarly, [25] investigated this domain, developing CO2 emission functions specifically for ICVs while incorporating time windows and partial recharging as additional model features.

[26] developed a mathematical model for the EVRP, which includes time windows and permits partial recharges. Their model also accounts for charging stations equipped with a variety of chargers, including normal, fast, and super-fast options, with the objective of minimizing both charging costs and the number of vehicles required. Given the lengthy durations required for recharging at stations, [27] explored an innovative approach. They proposed using this recharging time to facilitate customer visits by employing alternative transport modes such as bikes, drones, and segways. Their findings indicated a reduction in total recharging time, leading to a decrease in the overall distance traveled.

[28] introduced a mathematical model for the EVRP that accommodates split delivery, giving EVs greater flexibility in fulfilling customer demands. In their model, EVs can be partially charged and return to the depot for multiple trips. [29] focused on heterogeneous EVs, allowing for partial recharges at charging stations while implementing a fixed time charging at the depot.

[30] studied the consistent EVRP with backhauls, dividing each job into two sub-jobs: deliveries in the morning and pickups in the afternoon. [31] proposed two mathematical models for EVRP with partial and full recharge policies. Although their work primarily concentrated on methodology, the models show similarities to previous studies. [32] focused on the state of charge of EV batteries. They proposed a model that allows for partial recharging while maintaining the battery level between 25%-85% of its capacity. This approach is designed to prevent battery degradation and extend battery life.

While it is recognized that the charging function for electric vehicles is nonlinear, much of the EVRP literature simplifies this by considering a constant or

linear charging function for ease of handling [2], [4], [13], [14], [15]. The charging process is generally divided into two phases: the first being constant and increasing linearly with time, and the second where the current drops exponentially [33].

[34] explored the EVRP with a nonlinear charging function, employing a piecewise linear approximation to model the charging process. Similarly, [35] proposed an EVRP mathematical model incorporating a nonlinear charging function, enhancing the approach from [34] by using arc-based tracking variables.

Most electric vehicles use lithium-ion batteries, which are relatively costly to replace in full. [9], [10] conducted studies on the charging patterns of plug-in hybrid electric vehicles (PHEVs). Their findings indicate that higher storage States of Charge (SoC) accelerate battery degradation [9]. Furthermore, [10] reported that maintaining a charge of 90% or higher for over 80% of the time significantly reduces battery life. Clearly, the charging pattern has a profound impact on battery degradation.

[36] studied the EVRP with SoC and charging capacity constraints. The authors also proposed an efficient algorithm for large-scale EVRP instances. Their approach decomposes the original problem into three sequential subproblems — vehicle routing, charging station insertion, and charging scheduling — each formulated as a linear program, guaranteeing efficient computation and local optimality.

In practice, accommodating a lunch break for employees during the workday is a necessity, and this has been considered in various VRP studies. For instance, [6], [37] examined the waste collection VRP with time windows, explicitly incorporating drivers' lunch breaks. Their study included case studies from North America and Denmark, each necessitating different lunch break conditions. [38] explored the heterogeneous VRP in the context of home healthcare services, where caregivers, while servicing patients, are also provided with a lunch break. Furthermore, [8] integrated lunch break constraints into the VRP for the furniture delivery industry.

In the area of EVRP, studies that consider drivers' lunch breaks are relatively scarce, and those that do have varied policies regarding these breaks. [39] focused on EVRP, mandating that all assigned vehicles take their lunch breaks at restaurants equipped with charging facilities. Here, the charging level is set to the maximum battery capacity, incurring associated costs for both food and recharging services. As previously mentioned, [30] approached this differently by assigning two sub-jobs to each driver. Thus, after completing deliveries, drivers return to the depot for a partial recharge of their EVs, utilizing this interval as their lunch break.

EVRP is considered NP-hard as it is a generalization of VRP [40], [41], [42]. Consequently, many studies have developed heuristic methods to tackle the EVRP. [43] proposed the improved differential evolution algorithm to optimize EVRP with partial recharging policy and nonlinear charging. [44] proposed the two-phase heuristic method to solve EVRP for postal delivery and waste collection. The first phase clusters customer nodes to minimize total cost, and the second determines the routing strategy. Charging stations may be inserted at this phase if necessary. [45] integrated Ant Colony optimization (ACO) algorithm and deep heuristic information to solve the EVRP.

K-means is one of the solution approaches used in many works to deal with a large VRP [45], [46], [47]. The idea is to group customer nodes into a specific number of clusters $k$. Instead of grouping a set of customers, [48] applied K-means to group charging stations based on geographical proximity. This is to reduce the search space and improve computational efficiency. The initial step in K-means clustering requires specifying the value of $k$. However, determining the optimal value of $k$ remains a significant challenge. Consequently, researchers have increasingly focused on developing methodologies to identify the optimal $k$ value that produces the most satisfactory clustering results. In 2003, [49] introduced G-means, an algorithm that employs a statistical test to evaluate the hypothesis that a cluster follows a Gaussian distribution. [50] proposed the evaluation function $f(K)$ to assist researchers in determining the optimal value of $k$.

For a more comprehensive understanding of EVRP variants and their applications, readers are encouraged to consult additional resources such as [11], [12], [51]. More recently, [52] proposed a novel mixed-integer linear programming (MILP) formulation and a simulated annealing-based heuristic specifically for the VRP with time windows and lunch break (VRPTW-LB), demonstrating improved solution quality over existing MILP formulations for this class of problems. In the context of mixed fleet routing, [53] studied a bi-objective mixed-fleet VRP within a collaborative logistics framework, incorporating time windows and time-of-use electricity pricing to balance cost reduction with carbon emission targets. Furthermore, [54] examined mixed-fleet routing for cold chain logistics using diverse recharging strategies, demonstrating that a mixed fleet outperforms a homogeneous fleet in both cost and carbon emissions. Additionally, [55] investigated the mixed-fleet VRP with Low Emission Zones (LEZ), showing that urban access restrictions for ICVs significantly influence routing decisions in favor of EVs.

## 1.3 Scientific contribution

In this work, we study EVRP in which a mixed fleet of EVs and ICVs is considered. We assume that lunch

break is a mandatory stop for all drivers and must be taken place within specific time windows. Since ICV drivers do not need refueling during the day, they can stop at any location between two nodes according to the plan route. Some EV drivers may not need to charge their vehicles. Thus their condition for lunch break is the same as ICV drivers. For EV drivers who need to charge the vehicles, we encourage the drivers to visit CS during lunch break time windows. The aim is to take advantage of the idle time during drivers' lunch breaks by coordinating it with recharging time. In the context of Thailand, charging stations are usually located in petrol stations. Facilities may include restaurants, toilets and convenience stores. Therefore, drivers can rest, eat and relax while EVs are being charged. Additionally, charging stations provide multiple chargers so it is possible that several EVs could visit the same CS simultaneously.

The objective of the proposed MIP model is to minimize several cost factors: total distance travelled costs for both Electric Vehicles (EVs) and Internal Combustion Vehicles (ICVs), charging costs, and time-related expenses incurred at charging stations.

Therefore, in our study, we propose a method integrating CPLEX solver and clustering algorithm to optimize delivery routes for a mixed vehicle fleet, aiming to reduce overall costs while prioritizing the utilization of electric vehicles (EVs).

# 2 Problem Formulation

This section gives an explanation of the work. Subsequently, we introduce the mathematical programming model of the mixed fleet vehicle routing problem with a lunch break and partial charging.

## 2.1 Problem description

Our problem is defined on a directed graph $G = (V'_{0,n+1}, A)$ where $A = \{(i,j)|i,j \in V'_{0,n+1}, i \neq j\}$ represents the set of arcs. We have two types of vehicles: Electric Vehicles (EVs) and Internal Combustion Engine Vehicles (ICVs). These vehicle types have the same capacities; vehicles of the same type share homogeneous characteristics. The fleet size is limited but can cover the total demand. Hence it is not necessary to assign all available vehicles. On any given day, each vehicle is assigned to meet customers with specific demands and time windows, ensuring that the total goods delivered do not exceed the vehicle's capacity. Noting that split delivery is not permitted in this problem. For EVs, it is assumed that the battery capacity is full upon departure from the depot. Table 1 (Appendix) summarizes notations and definitions of the sets, parameters, and variables used in our model. It should be noted that a set denoted with subscript 0 or $n+1$ includes both the set itself and the depot, such that $V_{0,n+1}$ comprises the customer set $V$ and the depot vertices 0 and $n+1$.

To travel from one vertex to another, it is assumed that EVs consume energy at a constant rate of $h$ per kilometer. During their journey, EVs may need to visit charging stations to recharge. In this problem, there are two charging technologies, each with different charging costs and durations. The charging duration can be estimated from the amount of energy required and the charging rate of the charger, simplified as $\frac{z_{itk}}{g_t}$. EVs can recharge their batteries to any level, provided they have sufficient energy for the next leg of their route, whether visiting the next customer or returning to the depot. Although to follow the guideline for extending battery longevity, we set that the recharging battery must be between 25% to 80% of its capacity. In order to reduce the wait while charging, it is recommended to charge the vehicle during the lunch hour. Consequently, when scheduling stops at charging stations, the duration must account for the longer of the two activities: the charging time or the lunch break.

Alternatively, if the vehicle possesses sufficient energy for the entire route, drivers have the flexibility to take their lunch break at any preferred location between customer nodes $i$ and $j$. As a result, no supplementary driving or energy expenditure to the rest point is required to be considered.

## 2.2 Mathematical formulation

From the above problem description, we formulate a mathematical model for the EVRP with lunch break as follows. Firstly, each constraint is presented individually. The objective function will be displayed after all the constraints.

**Visit assignment constraint**

$$\sum_{i \in V'_0} \sum_{k \in M_{EV}} x^E_{ijk} + \sum_{i \in V_0} \sum_{k \in M_{IC}} x^{IC}_{ijk} = 1, \ \ \forall j \in V \quad (1)$$

The constraint (1) is to guarantee that all customers must be visited by a vehicle. The vehicle to visit a customer can be an EV, denoted by decision variable $x^E_{ijk}$ or ICV, denoted by decision variable $x^{IC}_{ijk}$.

**Vehicle management constraints**

$$\sum_{j \in V'} x^E_{0jk} \leq 1, \quad \forall k \in M_{EV} \quad (2)$$

$$\sum_{j \in V} x^{IC}_{0jk} \leq 1, \quad \forall k \in M_{IC} \quad (3)$$

$$\sum_{j \in F} \sum_{i \in V} x^E_{ijk} \leq 1, \quad \forall k \in M_{EV} \quad (4)$$

The vehicle management constraints consist of three inequalities, (2-4). The first two constraints (2)-(3) ensure that each vehicle is assigned at most

once and the assigned vehicles must start their journey from the depot. Constraint (4) limits the visiting times of the EVs so that each EV $k \in M_{EV}$ may visit a charging station $j \in F$ no more than one time.

**Flow constraints**

$$\sum_{j \in V'_{n+1}} x^E_{ijk} - \sum_{j \in V'_0} x^E_{jik} = 0, \quad \forall i \in V', k \in M_{EV} \tag{5}$$

$$\sum_{j \in V_{n+1}} x^{IC}_{ijk} - \sum_{j \in V_0} x^{IC}_{jik} = 0, \quad \forall i \in V, k \in M_{IC} \tag{6}$$

Constraints (5)-(6) guarantee that the number of incoming and outgoing arcs made by each vehicle type must be equal. These constraints were used in the majority of VRP models, [18], [25].

**Vehicle capacity constraints**

$$\sum_{j \in V} \sum_{i \in V'_0} q_j \cdot x^E_{ijk} \leq Q^E, \quad \forall k \in M_{EV} \tag{7}$$

$$\sum_{j \in V} \sum_{i \in V_0} q_j \cdot x^{IC}_{ijk} \leq Q^{IC}, \quad \forall k \in M_{IC} \tag{8}$$

Constraints (7)-(8) are the capacity constraint restrictions, showing that the total demand of each route must not exceed the vehicle capacities.

**Sub-tour elimination constraints for ICVs**

$$\tau_{ik} + (s_i + t_{ij}) \cdot x^{IC}_{ijk} + D \cdot y_{ik} - M(1 - x^{IC}_{ijk}) \leq \tau_{jk}, \quad \forall i \in V_0, j \in V_{n+1}, k \in M_{IC} \tag{9}$$

Constraints (9) is a sub-tour elimination constraint for ICVs to avoid assignment cycles. That is, if a vehicle $k$ is assigned to travel from location $i$ to $j$ ($x^{IC}_{ijk} = 1$), it means that the arrival time $\tau_{jk}$ at location $j$ must be at least the sum of the arrival time $\tau_{ik}$ at location $i$, service time $s_i$ at location $i$, travel time $t_{ij}$ from $i$ to $j$ and lunch break time $y_{ik}$ at location $i$ (if lunch break is applied at location $i$). Nothing that if $x^{IC}_{ijk} = 0$ and $M$ is a large enough constant, then the constraint will always be valid.

**Sub-tour elimination constraints for EVs**

$$\tau_{ik} + (s_i + t_{ij}) \cdot x^E_{ijk} + D \cdot y_{ik} - M(1 - x^E_{ijk}) \leq \tau_{jk}, \quad \forall i \in V_0, j \in V'_{n+1}, k \in M_{EV} \tag{10}$$

$$\tau_{ik} + (W_{ik} + t_{ij}) \cdot x^E_{ijk} - M(1 - x^E_{ijk}) \leq \tau_{jk}, \quad \forall i \in F, j \in V'_{n+1}, k \in M_{EV} \tag{11}$$

The constraints for EVs are structured similarly to those for ICVs. Specifically, Constraint (10) is formulated in the same way as Constraint (9). Meanwhile, Constraint (11) extends the formulation by including a term that accounts for an EV $k \in M_{EV}$ recharging its battery at charging station $i$.

**Time window constraints**

$$e_i \sum_{j \in V'_0} x^E_{jik} \leq \tau_{ik} \leq l_i \sum_{j \in V'_0} x^E_{jik}, \quad \forall i \in V, k \in M_{EV} \tag{12}$$

$$e_i \sum_{j \in V_0} x^{IC}_{jik} \leq \tau_{ik} \leq l_i \sum_{j \in V_0} x^{IC}_{jik}, \quad \forall i \in V, k \in M_{IC} \tag{13}$$

Constraints (12)-(13) ensure that the arrival time $\tau_{ik}$ at vertex $i$ must be assigned between the required time window.

**Lunch break constraints**

$$\sum_{j \in V} y_{jk} = \sum_{j \in V} x^{IC}_{0jk} \quad \forall k \in M_{IC} \tag{14}$$

$$\sum_{j \in V'} y_{jk} = \sum_{j \in V'} x^{EV}_{0jk} \quad \forall k \in M_{EV} \tag{15}$$

$$y_{jk} \leq \sum_{i \in V_0} x^{IC}_{ijk} \quad \forall j \in V, k \in M_{IC} \tag{16}$$

$$y_{jk} \leq \sum_{i \in V_0} x^{EV}_{ijk} \quad \forall j \in V', k \in M_{EV} \tag{17}$$

Constraints (14)-(15) ensure that the assigned vehicles must take exactly one lunch break. To be specific, if vehicle $k$ is used or departs from the depot (the right-hand side of (14)-(15) equals 1), therefore $y_{jk} = 1$ which means exactly one lunch break for vehicle $k$. To determine the location for lunch break, Constraints (16)-(17) guarantee that lunch break can only take place at location $j$ ($y_{jk} = 1$) only when vehicle $k$ is assigned to travel from location $i$ to $j$ (the right-hand side of (16)-(17) equals 1). Conversely, if vehicle $k$ does not visit location $j$ (the right-hand side of (16)-(17) equals 0), it forces $y_{jk}$ to be zero.

**Lunch break time window constraints**

$$E + D + t_{ij} \cdot x^{IC}_{ijk} - M(2 - y_{ik} - x^{IC}_{ijk}) \leq \tau_{jk}, \quad \forall i \in V_0, j \in V_{n+1}, k \in M_{IC} \tag{18}$$

$$\tau_{ik} + s_i \cdot x^{IC}_{ijk} - M(2 - y_{ik} - x^{IC}_{ijk}) \leq L, \quad \forall i \in V_0, j \in V_{n+1}, k \in M_{IC} \tag{19}$$

$$E + D + t_{ij} \cdot x^E_{ijk} - M(2 - y_{ik} - x^E_{ijk}) \leq \tau_{jk}, \quad \forall i \in V'_0, j \in V'_{n+1}, k \in M_{EV} \tag{20}$$

$$\tau_{ik} + s_i \cdot x^E_{ijk} - M(2 - y_{ik} - x^E_{ijk}) \leq L, \quad \forall i \in V', j \in V'_{n+1}, k \in M_{EV} \quad (21)$$

We assume that all drivers must take a lunch break during the day. In particular, lunch break must be taken under the specific time window $[E, L]$. Also, lunch break duration is limited, denoted by $D$. Therefore, we implement Constraints (9)-(11) to fit the lunch break condition, and they become Constraints (18) and (20). Constraints (19) and (21) define that lunch break must take place within its time window.

**Linking constraints**

$$\sum_{t \in T} z_{itk} \leq M \cdot y_{ik}, \quad \forall i \in F, k \in M_{EV} \quad (22)$$

$$D \cdot y_{ik} + \delta_{ik} = W_{ik}, \quad \forall k \in M_{EV}, i \in F \quad (23)$$

$$\sum_{t \in T} \frac{z_{itk}}{g_t} \leq W_{ik}, \quad \forall k \in M_{EV}, i \in F \quad (24)$$

This model includes a particular requirement for EVs when visiting charging stations: drivers are mandated to take their lunch breaks at the charging station if their vehicle is being charged. Consequently, we introduce Constraint (22), linking variables $z_{itk}$ and $y_{ik}$. Essentially, if there is a positive recharging energy $z_{itk}$ at charging station $i$ for vehicle $k$, then the vehicle must take a lunch break there. Given that the duration of lunch breaks and charging times can differ, we prioritize the longer of the two time slots to determine the time vehicle $k$ spends at charging station $i$. For instance, with a fixed lunch break of 60 minutes and a charging time of 30 minutes, the time spent at the station is considered to be 60 minutes, i.e., $W_{ik} = 60$. Conversely, if the charging time extends to 80 minutes, then $W_{ik} = 80$. Thus, Constraints (23)-(24) specify the duration EVs spend at charging stations, taking into account the longer of the two activities. In particular, the slack $\delta_{ik}$ is added into Constraint (23) and considered as the difference between lunch break duration and recharging time. If $\delta_{ik} = 0$, it means that a recharging time is within the fixed lunch break duration. On the other hand, if $\delta_{ik} > 0$, this implies that the vehicle requires more charging time or the duration of charging time is outside the lunch break. Thus, we would like to minimize this amount, and this is done by the fourth component in the objective function (33).

**Recharging constraints**

$$0.25B \cdot \sum_{j \in V'_0} x^E_{jik} \leq E^a_{ik}, \forall i \in V'_{n+1}, k \in M_{EV} \quad (25)$$

$$E^l_{ik} \leq 0.8B, \quad \forall i \in F, k \in M_{EV} \quad (26)$$

$$E^a_{ik} = E^l_{ik}, \quad \forall i \in V, k \in M_{EV} \quad (27)$$

$$E^a_{jk} \leq E^l_{ik} - h \cdot d_{ij} \cdot x^E_{ijk} + M(1 - x^E_{ijk}), \quad \forall i \in V'_0, j \in V'_{n+1}, k \in M_{EV} \quad (28)$$

$$E^a_{ik} + \sum_{t \in T} z_{itk} = E^l_{ik}, \quad \forall i \in F, k \in M_{EV} \quad (29)$$

$$E^l_{0k} = B, \quad \forall k \in M_{EV} \quad (30)$$

$$x^E_{ijk}, x^{IC}_{ijk}, y_{ik} \in \{0, 1\}, \quad \forall i, j \in V'_{0,n+1}, k \in M' \quad (31)$$

$$\tau_{ik}, z_{itk}, E^a_{ik}, E^l_{ik} \geq 0, \quad \forall i \in V'_{0,n+1}, k \in M', t \in T \quad (32)$$

Constraints (25)-(26) are established to regulate the battery levels, stipulating that the battery must not fall below 25% of its capacity nor exceed 80% during charging to extend battery life. Additionally, constraint (27) ensures that the battery levels upon arriving at and departing from customer nodes must remain constant, ensuring a stable state. Constraint (28) guarantees that an EV has sufficient energy for travel between connected vertices $i$ and $j$. Constraint (29) details the total energy an EV possesses upon completing the recharging process. Constraint (30) ensures that each EV begins its route with a fully charged battery. Finally, constraints (31)-(32) specify the domain of the variables.

**Objective function**

$$\begin{aligned} \text{min. } & cost^E \sum_{i \in V'_0} \sum_{j \in V'_{n+1}} \sum_{k \in M_{EV}} d_{ij} \cdot x^E_{ijk} \\ & + cost^{IC} \sum_{i \in V_0} \sum_{j \in V_{n+1}} \sum_{k \in M_{IC}} d_{ij} \cdot x^{IC}_{ijk} \\ & + c^t \sum_{j \in F} \sum_{t \in T} \sum_{k \in M_{EV}} z_{jtk} + \sum_{k \in M_{EV}} \sum_{i \in F} \delta_{ik} \end{aligned} \quad (33)$$

The objective function (33), measured in monetary units, is to minimize four costs: (i) the total traveling cost for EVs, (ii) the total traveling cost for ICVs, (iii) the charging cost of EVs at the charging stations, and (iv) the cost of charging vehicles outside lunch break duration.

## 2.3 Description of Instances

This section describes the instances utilized in this study, derived from an original dataset provided by a parcel delivery company operating in Bangkok metropolitan area. While the dataset includes features such as time windows, customer addresses, demand specifics, and a homogeneous vehicle fleet, it does not fully align with all our assumptions. Consequently, we have made necessary adaptations to this real-world dataset to ensure compatibility with our problem's unique requirements.

The dataset comprises a list of customers. The majority of customers are located in the central business district. Our initial step involved grouping customers sharing the same address into a single customer node. Subsequently, to align with our focus on the mixed fleet vehicle routing problem (VRP), we augmented the vehicle fleet with a set of electric vehicles. Finally, we incorporated a set of charging stations based on actual locations in Thailand.

After the adaptations, we categorized our instances into three groups based on the number of customers: Group A (up to 10 customers), Group B (between 11-50 customers), and Group C (more than 50 customers). Our dataset comprises 34 instances in total, consisting of 10 instances in Group A, 15 in Group B, and 9 in Group C. Table 2 details the overall characteristics of each instance, including the number of customers and the composition of the vehicle fleet. We adopted a naming convention for each instance as follows: the group of the instance (A, B, C), followed by the number of charging stations (CSs), and then the sequence number of the instance. For example, 'A101' denotes Group A instance, with '1' indicating the presence of one charging station, and '01' specifying its sequence.

Moreover, when two or more instances share the same group and sequence number, they also share common attributes, such as the number of customers, customer data, and vehicle count. The primary difference is the number of charging stations. For example, 'A101' and 'A201' both have the same sequence '01', meaning they have the same customer data and vehicle composition but differ in the number of charging stations: 'A101' has one charging station, while 'A201' has two charging stations.

Table 2. Characteristics of each instance

| Instance | # of customers | # EVs | # ICVs |
|---|---|---|---|
| A101, A201 | 7 | 2 | 2 |
| A102, A202 | 6 | 4 | 3 |
| A103, A203 | 10 | 3 | 4 |
| A104, A204 | 7 | 3 | 4 |
| A105, A205 | 9 | 3 | 4 |
| B101, B201, B301 | 12 | 3 | 3 |
| B102, B202, B302 | 20 | 6 | 7 |
| B103, B203, B303 | 19 | 4 | 7 |
| B104, B204, B304 | 50 | 5 | 5 |
| B105, B205, B305 | 30 | 5 | 5 |
| C101, C201, C301 | 60 | 5 | 5 |
| C102, C202, C302 | 55 | 8 | 8 |
| C103, C203, C303 | 75 | 10 | 10 |

*Source: created by the authors.*

# 3 Results and discussion

We organize our experiments into three sets. First, we solve the proposed problem using the mathematical programming model presented in subsection 2.2 and report the optimality gap. Second, we examine the effect of lunch break constraints to assess whether their inclusion makes the problem harder to solve. Lastly, we investigate the time required to obtain feasible solutions. All experiments were conducted using CPLEX 20.1.0 on a computer with Intel Core i7-1165G7 2.8 GHz CPU and 16 GB of RAM.

## 3.1 Feasibility and Optimality

In general, real-world industries need to quickly deal with changing circumstances or solve unique challenges on a daily or even hourly basis so that obtaining a solution after several hours of computation is impractical. Therefore we set a 15-minute time limit to test how CPLEX handles problems of different sizes under tight time constraints. For each instance with at least one feasible solution, we record two metrics: the time to the first feasible solution and the optimality gap when the solver hits the time limit.

In this experiment, only 6 out of 34 instances achieved optimality within 15 minutes, all of which are Group A instances. Table 3 lists these six instances along with the time at which the first feasible and optimal solutions were found. Most of these instances could be solved quickly as they contain a few customer nodes. Meanwhile, 16 instances were able to identify at least one feasible solution. For the remaining 12 instances, particularly all Group C and some Group B instances, no feasible solutions were found within the given time limit. Specifically, instances B104, B204, and B304 are the only instances from Group B that the solver could not solve within 15 minutes. This difficulty arises because these instances contain the largest number of customer nodes among Group B, which have 50 customers. Therefore, it is getting harder for a solver to tackle instances with at least 50 customer nodes.

Table 3. Computation Times (in seconds) for CPLEX to find the first feasible solution and optimal solution for instances in Group A

| Instance | A101 | A102 | A104 | A201 | A202 | A204 |
|---|---|---|---|---|---|---|
| First feasible | 0.4 | 0.16 | 0.58 | 0.46 | 0.53 | 0.28 |
| Optimal | 26 | 1.24 | 8 | 290 | 7 | 54 |

*Source: created by the authors.*

## 3.2 Effect of Lunch Break Constraints

To isolate the effect of lunch break constraints on computational difficulty, we re-solved the instances from subsection 3.1 with those constraints removed while leaving every other parameter unchanged. Drivers therefore take no break during the day. We kept the 15-minute CPLEX time limit for Group A instances and extended to 3 hours for Group B and C instances. Again, we recorded the time to the first feasible solution and the number of solvable instances. If the lunch break requirement is a meaningful source of difficulty for the mathematical

programming model, this relaxed variant should solve more instances and reach feasibility faster.

Table 4 presents the number of instances in each group where a solver found at least one feasible solution. The table consists of two rows: the first row shows the outcomes of the experiment with lunch break constraints (subsection 3.1), while the second row displays the number of solvable instances without the lunch break constraints. The result shows that the number of solvable instances is the same for both problems. This is not enough to conclude the difficulty of lunch break constraints and hence we also report the time (in seconds) taken by the solver to find the first feasible solution in Table 5 (Appendix). We do not report the results of B104, B204, B304 and Group C instances in this table as a solver found no solution for all of them.

The result shows that 15 out of 22 instances without lunch break constraints were solved faster by the solver, representing 68% of the cases. These results support our hypothesis that incorporating lunch break constraints increases the computational difficulty of the problem.

Table 4. Number of instances in which at least a feasible solutions is achieved.

| Lunch break constraints (LB) | Computational time (min) | Group A | Group B | Group C | Total |
|---|---|---|---|---|---|
| problem w/ LB | 15 | 10/10 | 12/15 | 0/9 | 22/34 |
| problem w/o LB | 15 | 10/10 | 12/15 | 0/9 | 22/34 |

*Source: created by the authors.*

An additional finding is that adding lunch-break constraints sometimes helps the solver achieve a tighter optimality gap rather than widening it. In 5 out of 12 solvable Group B instances (B103, B202, B203, B303, B305), the MIP gap under the LB model is lower than under the no-LB model. The most pronounced cases are B103 (gap reduced from 27.97% to 16.56%) and B303 (from 30.00% to 16.42%). This counter-intuitive result suggests that the lunch-break constraints narrow the feasible region in a way that guides the branch-and-bound search toward better incumbent solutions. These constraints therefore act as implicit valid inequalities in some problem structures, providing an additional rationale for including operationally motivated constraints in the formulation.

Exclusively focus on the costs in Table 6 (Appendix) and Table 7 (Appendix), we compare the objective value, distance, a number of stops (#stop), a number of used EVs (#EV) and ICVs (#ICV), and optimality gap for problems with and without lunch break constraints. Note that, in Table 6 (Appendix), the objective values with * indicate optimal solutions obtained by CPLEX. Meanwhile solutions with ** state that the obtained objective value is also optimal but, for some integer variables, CPLEX returns fractional values. However, they are considered feasible if the different between an integer and the obtained value is within the integrality tolerance. The default setting for integrality tolerance is 1.0e-5 or 0.00001. The solutions without any asterisks indicate the final feasible solutions when the solver reaches the time limit. The last column "%gap" in each block represents the relative MIP gap tolerance when CPLEX terminates. It measures the difference between the incumbent solution and the best bound.

According to Table 6 (Appendix), we can see that for group A instances the results of both problems are the same. Also, the planned routes found by CPLEX are identical. However, the solver achieved the better overall gap (approximately 3%) for the problem without lunch break constraints. Moreover, our solutions for Group A instances exclusively employ only EVs because of two key reasons: (1) the cost of using EVs is lower than the cost of ICVs, and (2) the fleet size and capacity of EVs are sufficient to meet customer requirements. The average distance traveled by each EV is 37.6 km. Therefore, the total distance traveled by each EV remains within their operational limits.

For Group B instances, none of the 15 instances reached optimality within the time limit (3 hours). Therefore, we reported the final feasible solution when the solver hits the time limit as shown in Table 7 (Appendix). When lunch break constraints are relaxed, 7 out of 12 instances achieved better gap although the average gap of the problem without lunch break constraints is slightly higher than the average gap of the problem with these constraints.

Furthermore, the objective value of the problem with lunch break constraints is slightly different from the results of the problem without lunch break constraints. CPLEX yields better objective value for the original problem which accounts for 7 out of 12 instances. Likewise, the distance follows the same trend as the objective value but the differences are only a few kilometers. Finally, the planned routes from CPLEX are totally different.

The main difference is charging behavior. Some instances, for example B201, B203 and B301, with lunch break constraints have charging plans for EV when the battery reaches limitation. These stops occur within lunch break time windows and synchronize the two activities as stated in our assumption. Meanwhile, when the lunch break constraints are removed, no EV visits charging stations during the day. Instead, ICVs are employed to complete the tasks for longer routes. Therefore, the objective value is increased because the operation cost for ICCVs is more expensive and much higher than charging cost.

More importantly, the results reveal that synchronizing EV recharging with mandatory

driver lunch breaks delivers measurable cost savings. Among the four instances where the LB-constrained model assigns a mid-route charging stop (B201, B203, B301, B302), three instances achieve a lower total objective value than their no-LB counterpart. B201 and B301 each save 47.47 THB (2.8%) by enabling an additional EV in place of an ICV through the synchronized charging window. B203 also reports a lower LB objective (1,369.30 THB, 3 EVs, 0 ICVs) than its no-LB counterpart (1,563.75 THB, 14.2% more expensive); however, B103 – which shares identical customer data with B203 (Table 2) but has fewer charging stations available – independently reaches a lower objective (1,309.39 THB) using the same fleet composition and no charging stop at all, a solution that remains feasible for B203 as well. This indicates the reported B203 incumbent, while a genuine feasible solution within the 3-hour time limit, was not the best available, and the specific magnitude of B203's synchronization benefit should be interpreted with caution pending a longer solver run. Across all solvable Group B instances, the LB model assigns 46 EV-routes versus 42 in the no-LB model, confirming a systematic shift toward greener fleet utilization when the lunch-break synchronization constraint is active.

In conclusion, lunch break constraints do not affect the instances with less than or equal ten customer nodes as the results (computational time, costs and vehicle routes) of Group A instances are almost identical. Although the computational results for Group B instances between problems with and without lunch break constraints are diverse, it is not significant to conclude that adding lunch break constraints influences the solver performance. In some cases such as instances B103, B203 and B203, CPLEX achieves significantly smaller gaps when lunch break constraints are considered. This finding suggests that additional constraints could guide CPLEX to improve the quality of solution. Hence integrating lunch breaks into EVRP can be practical without significantly compromising solution quality or computational performance.

For instances B104, B204, B304 and Group C instances, they remain unsolved even though we increase the computational time limit for both problems. Thus the difficulty does not come from the additional constraints but the characteristics themselves as these instances contain more than 50 customer nodes. It is challenging for CPLEX to handle large-scale instances.

## 3.3 Extending Computational Time

This experiment aims to expand upon the findings from subsection 3.1 by increasing the computational time. Thus, we set the time limits to 15, 60, and 180 minutes.

We extended the computation time to 60 minutes, but the results for the 12 unsolvable instances remained unchanged, even with more time allocated. Similarly, the solver did not achieve optimality for the remaining 16 instances, although it found additional feasible solutions.

Lastly, we increased the time limit to 180 minutes (or 3 hours), assuming that spending more than 3 hours solving the problem would be too time-consuming and impractical. The results were similar to those of the 60-minute experiment. However, the solver ran out of memory after 7,200 seconds for B105, after 9,000 seconds for B205 and B305, and after 10,800 seconds for C202.

## 3.4 Applying K-Means

The results shown previously confirmed the complexity of the proposed problem and hence cannot be tackled by the solver. To overcome this challenge, we employ the partition method, K-means, to partition our main problem. Finally, each partition is solved by the solver.

In this work, we develop a hybrid optimization framework that integrates K-means clustering decomposition with exact MIP optimization to address large-scale instances. The framework operates in three main stages:

### 3.4.1 Hybrid Optimization Architecture

1. Customer and Charging station Clustering: Customer nodes $i$ in $V$ and charging stations in $F$ are partitioned into $K$ spatial clusters based on their 2D geographical coordinates $(x_i, y_i)$.
2. Fleet & Infrastructure Allocation: The depot vertices (0 and $n+1$) are made accessible to all clusters. The available vehicle fleet ($M_{EV}$ and $M_{IC}$) is allocated as equally as possible among the $K$ clusters. Specifically, each cluster subproblem receives $\lfloor |M_{EV}|/K \rfloor$ electric vehicles and $\lfloor |M_{IC}|/K \rfloor$ internal combustion vehicles, with any remaining vehicles assigned sequentially.
3. Subproblem Optimization: Each cluster subproblem is solved independently using the MIP model (Equations 1-33) in CPLEX subject to a 15-minute (900-second) time limit. The global solution is formed by aggregating the sub-routes across all clusters.

### 3.4.2 Selection of Optimal Number of Clusters $K$

To determine the optimal number of clusters $K$ objectively, we adopt the evaluation function $f(K)$ proposed by [50]. The candidate values of $K$ range from 1 to the total fleet size $|M|$. For a given $K$, the metric $f(K)$ is defined as Equation (34):

$$f(K) = \begin{cases} 1 & \text{if } K = 1, \\ \frac{S_K}{\alpha_K S_{K-1}} & \text{if } S_{K-1} \neq 0, \forall K > 1, \\ 1 & \text{if } S_{K-1} = 0, \forall K > 1 \end{cases} \quad (34)$$

Here, $S_K$, Equation (35), is the sum of squared Euclidean distances between customer coordinates and their assigned cluster centroid:

$$S_K = \sum_{c=1}^{K} \sum_{i \in C_c} [(x_i - \bar{x}_c)^2 + (y_i - \bar{y}_c)^2] \quad (35)$$

and $\alpha_K$, Equation (36)-(37), is a 2D weight factor.

$$\alpha_2 = 1 - \frac{3}{4N_d} = \frac{5}{8} \quad (36)$$

$$\alpha_K = \alpha_{K-1} + \frac{1 - \alpha_{K-1}}{6}, \; K > 2 \quad (37)$$

[50] proved that values of $K$ that yield local minima of $f(K)$ represent natural, well-defined spatial clusters.

### 3.4.3 Algorithmic Procedure

Algorithm 1 outlines the complete procedure. In the first stage, we follow the method of [50] to find the number of clusters ($K^*$). We then apply the standard K-means to partition the set of geographical points, which is the union of a set of customers and a set of charging stations. The second stage is to assign the fleet of vehicles to each cluster equally.

The final stage is to solve each cluster independently by CPLEX. It is clear that we have limited charging stations and thus some clusters may not have CS. Clusters containing CS reserve the characteristics of EVRP with recharging decisions. In contrast, for clusters without CS, the subproblem is treated as VRP-type routing problem because no charging facility is available. EV routes can only be included when their associated routes satisfy the battery feasibility requirements without recharging. Finally, we combine each solution from all clusters to form the global solution.

The overall time complexity of this algorithm is split into two parts. For the 2-dimensional standard K-means, the time complexity is denoted by $O(nKi)$, where $n$ is the number of points, $K$ is the number of clusters, and $i$ is the number of iterations.

The latter part is the routing subproblem tackled by CPLEX which is considered NP-hard [40], [41], [42]. Therefore it cannot be fixed by Big O notation. Let $n_k$ be the number of points in cluster $k$ and $T(n_k)$ be the computational time for solving the $k$-th cluster. Thus the total computational time for this part is displayed by (38).

$$\sum_{k=1}^{K^*} T(n_k) \quad (38)$$

Consequently, the time complexity of this algorithm can be represented as (39)

$$O(nKi) + \sum_{k=1}^{K^*} T(n_k). \quad (39)$$

Since EVRP is a combinatorial optimization problem, splitting a large problem into smaller subproblems can dramatically reduce the search space. Thus, the hybrid optimization shifts the computational burden from a single large NP-hard problem to several smaller subproblems. In addition, if a cluster contains no charging station, it could further reduce its computational burden.

**Algorithm 1** Hybrid K-Means Decomposition and MIP Optimization

1: **for** $K = 1$ to $K_{\max}$ **do**
2: Execute K-means clustering on customer coordinates $(x_i, y_i)$
3: Calculate distortion $S_K$ and weight factor $\alpha_K$
4: Compute evaluation function $f(K)$
5: **end for**
6: Select optimal $K^* = \arg\min_K f(K)$
7: Partition a set $V \cup F$ into $K^*$ clusters $\{C_1, C_2, \ldots, C_{K^*}\}$
8: **for** each cluster $c = 1$ to $K^*$ **do**
9: Assign sub-fleet $M_{EV}^c$ and $M_{IC}^c$ equally
10: Solve sub-instance using CPLEX MIP model (Time limit = 900 s)
11: **end for**
12: Aggregate sub-routes into global delivery solution

### 3.4.4 Result analysis

The second column in Table 8 (Appendix) presents the best choice $K^*$ for each instance. Most instances are split into 2 or 3 clusters, whereas larger instances are divided into up to 8 clusters. The average number of customer nodes per cluster (column 3 of Table 8 (Appendix)) ranges from 1 to 30 nodes.

The visualizations for clustering approach are displayed in Figure 1 (Appendix). We show some results with $K^* = 2$ (A104 and C101), $K^* = 3$ (B205) and $K^* = 8$ (B105). Instances A104, B105, and B205 were equally partitioned according to their geographical locations. On the other hand, instance C101 was also split into two clusters but the number of customers in the clusters is 15 and 46 which results in an unbalanced distribution. Red markers indicate the location of charging stations. As there are 1-3 stations available, some clusters have no CS and cannot access the facility.

It is easy to see that instance A104 (Figure 1(a)) has two well-separated regions. $f(K)$ suggests the correct value of $K$. A charging station is assigned to cluster 1 and relatively close to its cluster center. The decomposition reflects the actual spatial distribution of the available charging station.

For instances B105, B205 and C101, the objects are not well-defined regions. Hence we perform a clustering with the suggested values $K^*$. For B105, the only one CS is assigned to cluster 5 near the boundary of the region. Meanwhile, two CS of instance B205 are inserted to different clusters according to their geography. Instance C101 has exactly one CS and it is assigned to cluster 0 where it contains more customer nodes than another cluster.

Clearly, the selected $K^*$ from [50] produces geographically meaningful decompositions and the availability of charging stations in each cluster is a consequence of their actual geographical distribution. This feature is particularly relevant to the proposed EVRP because clusters containing charging stations can incorporate recharging decisions, whereas clusters without charging stations must satisfy the battery constraints without recharging.

Overall, the computational results from the clustering decomposition method yield feasible solutions for all clusters, as intended. In several cases—such as instances B102, B104, B205, and C102—the clustered subproblems reach optimal solutions. Notably, for smaller instances that already achieved optimal solutions in Section 3.1, the outcomes remain unchanged when applying the clustering decomposition method. Furthermore, by reducing the problem size, the solver was able to find feasible or optimal solutions within a short computation time.

When comparing the objective values and total distances between the problem with a lunch break and the results obtained using K-means clustering (Tables 6, Table 7 (Appendix) and Table 8(Appendix)), we found that the direct solver approach yields lower objective values than clustering for most instances. Exceptions include instances A103, B103, B203, and B302, where the clustered versions achieve comparable or better results, likely because the solver found optimal solutions for some of their clusters. In contrast, instances A105 and A205 show significantly higher objective values after clustering. This occurs because the number of clusters equals the number of available vehicles, obliging the solver to deploy every vehicle and thereby increasing total travel distance and cost.

However, a noteworthy counter-finding is that for several instances, the clustering decomposition actually produces a better objective value than the direct CPLEX solve within the same three-hour time limit. Specifically, B101 achieves 1,573.61 THB under clustering compared to 1,673.19 THB from the direct solve (a 6.0% improvement), B201 achieves 1,573.61 THB versus 1,625.72 THB (3.2% improvement) and B202 achieves 2,224.53 versus 2,264.88 THB (1.8% improvement). These results indicate that the clustering decomposition framework is not merely a feasibility tool for large-scale instances but can also improve solution quality for medium-scale instances where direct optimization reaches only a weak feasible solution within the time limit. By decomposing the problem into spatially coherent subproblems, CPLEX concentrates its branch-and-bound effort on a tighter search space, enabling it to find higher-quality incumbents before the time limit is reached.

To ensure that clustering technique improves the solution quality, i.e. the differences between results from CPLEX and hybrid K-means is positive, we perform the one-tailed Wilcoxon signed-rank test based on a significance level = 0.05 ($\alpha = 0.05$) as our sample is non-normally distributed data (see Figure 2 (Appendix)). Our hypothesis states that

$H_0$ :The median of the distribution of paired differences is nonpositive.

$H_a$ : The median of the distribution of paired differences is positive.

The result shows that the test statistic = 63.0 and the p-value = 0.9660 > 0.05. To conclude, we fail to reject the null hypothesis, meaning that we do not have enough evidence to say that the results from clustering have better quality than CPLEX.

When the solver accounts for the given limitations, we generally observe that each cluster is served exclusively by EVs. This is because (1) the EVs' combined capacity within the cluster is sufficient to meet customer demand, and (2) charging stations are located nearby, allowing EVs to recharge and continue their routes. However, in some clusters, both EVs and a few ICVs are used. This occurs when the total capacity of EVs alone is insufficient to meet demand, making it necessary to deploy ICVs to fulfill the remaining requirements.

### 3.5 Sensitivity Analysis on Battery State-of-Charge Bounds

To assess whether the 25%-80% state-of-charge (SoC) policy adopted throughout this study - chosen to preserve battery longevity following [8], [9], [10] - imposes a measurable routing-cost penalty relative to a wider operational window, we re-solved the Group A instances using the same mathematical model (Equations 1-33, unmodified except for the SoC bounds in Constraints (25) and (31)) under two additional windows: 10%-90% and 0%-100%. All three windows were solved fresh under an identical 15-minute time limit and the same solver (CPLEX 12.10) to ensure a fair, within-solver comparison; results are summarized in Table 9 (Appendix). To test whether this effect generalizes beyond small instances, we additionally re-solved the four Group B instances with a baseline charging stop (B201, B203, B301, B302) under the same three SoC windows, using a 60-minute time limit (matching Subsection 3.3's extended-time tier) with CPLEX configured for 2 threads per run to allow the four instances to be

solved in parallel; these results are included in Table 9 (Appendix) as well, with their own time limit noted in the table.

Widening the SoC window reduced the objective value for two of the ten Group A instances, A104 and A204, while leaving the remaining eight unchanged. The mechanism differs between the two cases. For A104, the 25%-80% solution requires one charging stop (633.21 THB); widening the window to 10%-90% or 0%-100% removes the need to charge altogether, reducing cost to 578.21 THB (-8.7%). For A204, no charging stop is used under any window, yet cost still falls from 675.04 THB to 578.21 THB (-14.3%) because the lower state-of-charge floor extends the maximum distance an EV can travel before its battery would fall below the minimum bound: with battery capacity $B = 10$ kWh and consumption rate $h = 0.2$ kWh/km, the reachable range without recharging is $\frac{(1-SoC_{min})*B}{h}$, i.e. 37.5 km at the 25% floor versus 45 km at 10% and 50 km at 0%. Extending this range lets the solver assign a more direct route without violating the minimum state-of-charge constraint at intermediate stops. The remaining eight Group A instances either never required the extra range at any window, or the 15-minute time limit returned the same incumbent solution regardless of window; four instances (A103, A105, A203, A205) did not reach proven optimality within the time limit under any window, with gaps reported in Table 9 (Appendix).

The same route-efficiency mechanism observed for A204 replicates across all four Group B instances, which are substantially larger (12-20 customers versus Group A's 6-10 customers): widening the SoC window from 25%-80% to 10%-90% reduced cost by 3.6-9.5%, and to 0%-100% by 7.6-12.5% (Table 9 (Appendix)). None of these Group B runs – at either the 15-minute or the 60-minute time limit – found a solution using a charging stop, unlike the original 3-hour runs reported in Table 7 (Appendix); consequently, unlike A104, none of the Group B rows in Table 9 (Appendix) involve eliminating a charging stop, and none reached proven optimality (MIP gaps of 10-37% are reported alongside each result). This indicates the cost benefit of a wider SoC window is not limited to charging avoidance – it applies directly to route efficiency for larger fleet-routing decisions as well. We additionally tested whether decoupling an EV's mandatory lunch break from its charging stop – permitting the 60-minute break to occur at a customer location as ICVs already do, while a charging stop costs only the time actually needed to recharge – changes the outcome, for the one Group A instance whose baseline solution uses a charging stop (A104). The objective was unchanged (633.21 THB under both policies), suggesting that for this instance the mandatory break already absorbs the required charging time at no additional cost. We attempted the same comparison for the four Group B instances at both a 15-minute and a 60-minute time limit; neither run found a charging-based solution for any Group B instance under either policy (consistent with the absence of charging stops noted above), so the synchronization mechanism itself remains untested at Group B scale. Testing it conclusively would require a time budget closer to the 3 hours used in Subsection 3.2, which was beyond what was available for this revision, and is left for future work.

Overall, this analysis indicates that the battery-longevity-preserving 25%-80% policy carries a real, bounded routing-cost penalty rather than being cost-neutral in general: up to 14.3% for the two Group A instances where it binds, and 3.6-12.5% across all four tested Group B instances, while for the remaining Group A instances the policy has no measurable cost impact. A full Group C sensitivity analysis, and a conclusive test of the lunch-break/charging synchronization mechanism at Group B scale, both require a longer per-instance time budget than was available for this revision and are left for future work.

# 4 Conclusion

This study proposed a mathematical programming model combined with a clustering decomposition method for a mixed-fleet vehicle routing problem involving both conventional and electric vehicles. The problem was further extended by incorporating mandatory lunch break constraints for all drivers. To validate the proposed model, a real dataset from a courier company in Thailand was adapted, yielding 34 instances grouped into three categories according to the number of customers: Groups A, B, and C.

Three sets of experiments were conducted to examine solution feasibility, the effects of lunch break constraints, and the benefits of extended computational time. In the first experiment, only six Group A instances (A101, A102, A104, A201, A202, and A204) reached optimality within the 15-minute time limit, while none of the Group C instances yielded feasible solutions. In analyzing the effect of lunch break constraints, we increased the time limit to 3 hours for a solver to solve both problems with and without lunch break constraints. The findings indicated that incorporating lunch break conditions has a little effect on the complexity. Moreover, additional constraints sometimes help a solver to search for better solutions.

To assess potential gains from additional computation, we extended the time limits to 60 and 180 minutes. Although some improvements were observed for problems that did not reach optimality within 15 minutes, several Group B and C instances still failed to produce optimal or feasible solutions. To address the scalability issue, we applied

K-means clustering to partition the original problems into smaller subproblems, which were then solved individually. This approach successfully produced feasible solutions for all instances. Notably, for some instances—such as A103, B103, B203, B301, and B302—the clustering method led to improved results, with the solver achieving optimal solutions in certain clusters.

To further examine the trade-off between battery longevity and routing cost, we tested two additional state-of-charge windows (10%-90% and 0%-100%) against the baseline 25%-80% policy for Group A and Group B instances (Subsection 3.5). Widening the window reduced routing cost by up to 14.3% for the Group A instances where the tighter window was binding, and by 3.6-12.5% across all four tested Group B instances, while leaving the remaining Group A instances unaffected.

From a practical standpoint, three key managerial insights emerge from the computational results. First, synchronizing EV charging with mandatory driver lunch breaks is economically beneficial: the lunch-break-constrained model reduces total delivery costs in the majority of medium-scale Group B instances and enables the deployment of more EVs, reducing reliance on expensive ICVs. Second, incorporating operational constraints such as lunch-break requirements does not necessarily increase computational difficulty; in several instances these constraints tightened the solver's optimality gap by up to 13.6 percentage points, demonstrating that real-world operational constraints can serve as effective surrogate valid inequalities. Third, for logistics operators with delivery zones exceeding 50 customer nodes, the K-means clustering decomposition approach is recommended as a practical alternative to direct exact optimization: it produced feasible solutions for all 34 tested instances including all 12 large-scale unsolved instances (the 9 Group C instances plus B104, B204, and B304 from Group B) for which the direct CPLEX solver could not find any feasible solution within three hours, while also outperforming the direct solver in solution quality for several medium-scale instances. Fourth, the 25%-80% battery-longevity policy carries a bounded routing-cost penalty – up to 14.3% for Group A instances and up to 12.5% for the larger Group B instances tested – rather than a negligible one – information operators can use this to weigh battery-life preservation against routing cost for their specific delivery patterns.

Future work should explore metaheuristic and hybrid methods, since exact solvers are insufficient for medium- and large-scale instances within a practical time frame. Several recent advances offer promising directions for extension to the mixed-fleet setting with lunch breaks: the improved differential evolution algorithm for EVRP with nonlinear charging [34], the two-phase heuristic for postal and waste-collection routing [44] and the ACO-based approach with deep heuristic information [45]. A more realistic energy consumption model also warrants study. Such a model should account for vehicle load, road gradient, weather, and traffic congestion.

**Declaration of Generative AI and AI-assisted Technologies in the Writing Process**

During the preparation of this work, the author(s) utilized artificial intelligence (AI) technologies solely for the purpose of linguistic refinement and grammatical correction. Following the application of these tools, the author(s) comprehensively reviewed, verified, and edited the resulting text. The author(s) maintain full accountability and responsibility for the accuracy, integrity, and final content of the publication.

*References:*

[1] Emma Graham and Lee Ying Shan. A timeline of how the iran war shook oil prices — and what comes next. https://www.cnbc.com/2026/04/21/oil-price-iran-war-middle-east.html, 2026. Accessed: 05-21-2026.

[2] Electric vehicle myths. https://www.epa.gov/greenvehicles/electric-vehicle-myths, 2026. Accessed: 07-15-2026.

[3] Ángel Felipe, M Teresa Ortuño, Giovanni Righini, and Gregorio Tirado. A heuristic approach for the green vehicle routing problem with multiple technologies and partial recharges. *Transportation Research Part E: Logistics and Transportation Review*, 71:111–128, 2014. https://doi.org/10.1016/j.tre.2014.09.003.

[4] Ryan G Conrad and Miguel Andres Figliozzi. The recharging vehicle routing problem. In *Proceedings of the 2011 industrial engineering research conference*, volume 8. IISE Norcross, GA, USA, 2011. URL http://web.cecs.pdx.edu/~maf/Conference_Proceedings/2011_The_Recharging_Vehicle_Routing_Problem.pdf. Accessed: 04-21-2025.

[5] Michael Schneider, Andreas Stenger, and Dominik Goeke. The electric vehicle-routing problem with time windows and recharging stations. *Transportation science*, 48(4): 500–520, 2014. https://doi.org/10.1287/trsc.2013.0490.

[6] Byung-In Kim, Seongbae Kim, and Surya Sahoo. Waste collection vehicle routing problem with time windows. *Computers & Operations Research*, 33(12):3624–3642, 2006. https://doi.org/10.1016/j.cor.2005.02.045.

[7] Yves Rochat and Frédéric Semet. A tabu search approach for delivering pet food and flour in switzerland. *Journal of the Operational Research Society*, 45(11): 1233–1246, 1994. https://doi.org/10.1057/jors.1994.197.

[8] Leandro C Coelho, Jean-Philippe Gagliardi, Jacques Renaud, and Angel Ruiz. Solving the vehicle routing problem with lunch break arising in the furniture delivery industry. *Journal of the Operational Research Society*, 67(5):743–751, 2016. https://doi.org/10.1057/jors.2015.90.

[9] Saeid Bashash, Scott J Moura, Joel C Forman, and Hosam K Fathy. Plug-in hybrid electric vehicle charge pattern optimization for energy cost and battery longevity. *Journal of power sources*, 196(1):541–549, 2011. https://doi.org/10.1016/j.jpowsour.2010.07.001.

[10] Benedikt Lunz, Zexiong Yan, Jochen Bernhard Gerschler, and Dirk Uwe Sauer. Influence of plug-in hybrid electric vehicle charging strategies on charging and battery degradation costs. *Energy Policy*, 46:511–519, 2012. https://doi.org/10.1016/j.enpol.2012.04.017.

[11] Tomislav Erdelić and Tonči Carić. A survey on the electric vehicle routing problem: variants and solution approaches. *Journal of Advanced Transportation*, 2019, 2019. https://doi.org/10.1155/2019/5075671.

[12] Mohammad Asghari and S Mohammad J Mirzapour Al-e. Green vehicle routing problem: A state-of-the-art review. *International Journal of Production Economics*, 231:107899, 2021. https://doi.org/10.1016/j.ijpe.2020.107899.

[13] Sevgi Erdoğan and Elise Miller-Hooks. A green vehicle routing problem. *Transportation research part E: logistics and transportation review*, 48(1):100–114, 2012. https://doi.org/10.1016/j.tre.2011.08.001.

[14] Merve Keskin and Bülent Çatay. Partial recharge strategies for the electric vehicle routing problem with time windows. *Transportation research part C: emerging technologies*, 65:111–127, 2016. https://doi.org/10.1016/j.trc.2016.01.013.

[15] Maurizio Bruglieri, Simona Mancini, Ferdinando Pezzella, Ornella Pisacane, and Stefano Suraci. A three-phase matheuristic for the time-effective electric vehicle routing problem with partial recharges. *Electronic Notes in Discrete Mathematics*, 58:95–102, 2017. https://doi.org/10.1016/j.endm.2017.03.013.

[16] Hyungbin Park and Sukho Jin. Electric vehicle routing problem with heterogeneous vehicles and partial charge. *International Journal of Industrial Engineering and Management*, 11(4):215–225, 2020. URL https://ijiemjournal.uns.ac.rs/index.php/ijiem/article/view/82. Accessed: 04-21-2025.

[17] Jane Lin, Wei Zhou, and Ouri Wolfson. Electric vehicle routing problem. *Transportation research procedia*, 12:508–521, 2016. https://doi.org/10.1016/j.trpro.2016.02.007.

[18] Ons Sassi, Wahiba Ramdane Cherif-Khettaf, and Ammar Oulamara. Vehicle routing problem with mixed fleet of conventional and heterogenous electric vehicles and time dependent charging costs. *World Academy of Science, Engineering and Technology, International Journal of Mathematical, Computational, Physical, Electrical and Computer Engineering*, 9:171–181, 2015. URL https://hal.science/hal-01083966/. Accessed: 04-21-2025.

[19] Gerhard Hiermann, Jakob Puchinger, Stefan Ropke, and Richard F Hartl. The electric fleet size and mix vehicle routing problem with time windows and recharging stations. *European Journal of Operational Research*, 252(3):995–1018, 2016. https://doi.org/10.1016/j.ejor.2016.01.038.

[20] Dominik Goeke and Michael Schneider. Routing a mixed fleet of electric and conventional vehicles. *European Journal of Operational Research*, 245(1):81–99, 2015. https://doi.org/10.1016/j.ejor.2015.01.049.

[21] VF Yu, Panca Jodiawan, Aldy Gunawan, and Audrey Tedja Widjaja. A mathematical programming model for the green mixed fleet vehicle routing problem with realistic energy consumption and partial recharges. In *2019 IEEE International conference on industrial engineering and engineering management (IEEM)*, pages 1339–1343, Macao, China, 2019. IEEE. https://doi.org/10.1109/IEEM44572.2019.8978715.

[22] Nisrine Mouhrim, Ahmed El Hilali Alaoui, and Jaouad Boukachour. Vehicle routing problem with mixed fleet of electric and conventional vehicles under emissions allowances. In *2018 4th International Conference on Logistics Operations Management (GOL)*, pages 1–5, Le Havre, France, 2018. IEEE. https://doi.org/10.1109/GOL.2018.8378100.

[23] Md Anisul Islam and Yuvraj Gajpal. Optimization of conventional and green vehicles composition under carbon emission cap. *Sustainability*, 13(12):6940, 2021.

https://doi.org/10.3390/su13126940.

[24] A El Bouzekri El Idrissi, M Elhassania, and AA El Hilali. A genetic algorithm for optimizing the amount of emissions of greenhouse gaz for capacitated vehicle routing problem in green transportation. *International Journal of Soft Computing*, 8 (6):406–415, 2013. URL https://www.makhillpublications.co/view-article/1816-9503/ijscomp.2013.406.415. Accessed: 04-21-2025.

[25] Giusy Macrina, Luigi Di Puglia Pugliese, Francesca Guerriero, and Gilbert Laporte. The green mixed fleet vehicle routing problem with partial battery recharging and time windows. *Computers & Operations Research*, 101:183–199, 2019. https://doi.org/10.1016/j.cor.2018.07.012.

[26] Merve Keskin and Bülent Çatay. A matheuristic method for the electric vehicle routing problem with time windows and fast chargers. *Computers & operations research*, 100:172–188, 2018. https://doi.org/10.1016/j.cor.2018.06.019.

[27] David L Cortés-Murcia, Caroline Prodhon, and H Murat Afsar. The electric vehicle routing problem with time windows, partial recharges and satellite customers. *Transportation Research Part E: Logistics and Transportation Review*, 130:184–206, 2019a. https://doi.org/10.1016/j.tre.2019.08.015.

[28] Nader Al Theeb, Mohammed Hayajneh, and Naqaa AL Qubelat. Optimization of logistic plans with adopting the green technology considerations by utilizing electric vehicle routing problem. *Industrial Engineering & Management Systems*, 19(4):774–789, 2020. https://doi.org/10.7232/iems.2020.19.4.774.

[29] Yuzhen Zhou, Jincai Huang, Jianmai Shi, Rui Wang, and Kuihua Huang. The electric vehicle routing problem with partial recharge and vehicle recycling. *Complex & Intelligent Systems*, 7(3):1445–1458, 2021. https://doi.org/10.1007/s40747-021-00291-3.

[30] Pamela C Nolz, Nabil Absi, Dominique Feillet, and Clóvis Seragiotto. The consistent electric-vehicle routing problem with backhauls and charging management. *European Journal of Operational Research*, 302(2):700–716, 2022. https://doi.org/10.1016/j.ejor.2022.01.024.

[31] Tomislav Erdelić and Tonči Carić. Goods delivery with electric vehicles: Electric vehicle routing optimization with time windows and partial or full recharge. *Energies*, 15(1):285, 2022. https://doi.org/10.3390/en15010285.

[32] Cristian Cataldo-Díaz, Rodrigo Linfati, and John Willmer Escobar. Mathematical model for the electric vehicle routing problem considering the state of charge of the batteries. *Sustainability*, 14(3):1645, 2022. https://doi.org/10.3390/su14031645.

[33] Samuel Pelletier, Ola Jabali, Gilbert Laporte, and Marco Veneroni. Battery degradation and behaviour for electric vehicles: Review and numerical analyses of several models. *Transportation Research Part B: Methodological*, 103:158–187, 2017. https://doi.org/10.1016/j.trb.2017.01.020.

[34] Alejandro Montoya, Christelle Guéret, Jorge E Mendoza, and Juan G Villegas. The electric vehicle routing problem with nonlinear charging function. *Transportation Research Part B: Methodological*, 103:87–110, 2017. https://doi.org/10.1016/j.trb.2017.02.004.

[35] Aurélien Froger, Jorge E Mendoza, Ola Jabali, and Gilbert Laporte. Improved formulations and algorithmic components for the electric vehicle routing problem with nonlinear charging functions. *Computers & Operations Research*, 104:256–294, 2019. https://doi.org/10.1016/j.cor.2018.12.013.

[36] Haoyu Miao, Shibo Chen, Mengfan Cao, and Zaiyue Yang. Efficient algorithm for large scale electric vehicle routing problem with charging capacity constraint. *IEEE Transactions on Intelligent Transportation Systems*, 26(10):16700–16709, 2025. https://doi.org/10.1109/TITS.2025.3585987.

[37] Katja Buhrkal, Allan Larsen, and Stefan Ropke. The waste collection vehicle routing problem with time windows in a city logistics context. *Procedia-Social and Behavioral Sciences*, 39:241–254, 2012. https://doi.org/10.1016/j.sbspro.2012.03.105.

[38] Mohamed Amine Masmoudi and Naoufel Cheikhrouhou. Heterogeneous vehicle routing problems with synchronization: application to homecare scheduling routing problem. In *GISEH 2018*, pages 1–8, Geneva, Switzerland, 2018. URL https://arodes.hes-so.ch/record/2574?v=pdf. Accessed: 04-21-2025.

[39] David L Cortés-Murcia, H Murat Afsar, and Caroline Prodhon. A branch and price algorithm for the electric capacitated profitable tour problem with mandatory stops. *IFAC-PapersOnLine*, 52(13): 1572–1577, 2019b. https://doi.org/10.1016/j.ifacol.2019.11.424.

[40] Anagnostopoulou Afroditi, Maria

Boile, Sotirios Theofanis, Eleftherios Sdoukopoulos, and Dimitrios Margaritis. Electric vehicle routing problem with industry constraints: trends and insights for future research. *Transportation Research Procedia*, 3:452–459, 2014. https://doi.org/10.1016/j.trpro.2014.10.026.

[41] Guy Desaulniers, Fausto Errico, Stefan Irnich, and Michael Schneider. Exact algorithms for electric vehicle-routing problems with time windows. *Operations Research*, 64(6):1388–1405, 2016. https://doi.org/10.1287/opre.2016.1535.

[42] Ilker Kucukoglu, Reginald Dewil, and Dirk Cattrysse. The electric vehicle routing problem and its variations: A literature review. *Computers & Industrial Engineering*, 161:107650, 2021. https://doi.org/10.1016/j.cie.2021.107650.

[43] Jiawen Deng, Jihui Zhang, and Shengxiang Yang. Optimizing electric vehicle routing with nonlinear charging and time windows using improved differential evolution algorithm. *Cluster Computing*, 27(4):5423–5458, 2024. https://doi.org/10.1007/s10586-023-04243-z.

[44] Maria Asuncion del Cacho Estil-Les, Agostino Marcello Mangini, Michele Roccotelli, and Maria Pia Fanti. Electric vehicle routing optimization for postal delivery and waste collection in smart cities. *IEEE Transactions on Intelligent Transportation Systems*, 26(3):3307–3323, 2025. https://doi.org/10.1109/TITS.2025.3529181.

[45] Chao Wang, Hua Zhang, Jin Wang, and Lei Zhang. Ant colony optimization with deep heuristic information for solving electric vehicle routing problems. *IEEE Internet of Things Journal*, 12(24):54436 – 54449, 2025. https://doi.org/10.1109/JIOT.2025.3620353.

[46] Ruhan He, Weibin Xu, Jiaxia Sun, and Bingqiao Zu. Balanced k-means algorithm for partitioning areas in large-scale vehicle routing problem. In *2009 Third International Symposium on Intelligent Information Technology Application*, volume 3, pages 87–90, Nanchang, China, 2009. IEEE. https://doi.org/10.1109/IITA.2009.307.

[47] Noha Mostafa and Amr Eltawil. Solving the heterogeneous capacitated vehicle routing problem using k-means clustering and valid inequalities. In *Proceedings of the International Conference on Industrial Engineering and Operations Management*, pages 2239–2249, Rabat, Morocco, 2017. URL https://ieomsociety.org/proceedings/morocco2017/519.pdf. Accessed: 04-21-2025.

[48] Tal Gaon, Yovel Gabay, and Miri Weiss Cohen. Optimizing electric vehicle routing efficiency using k-means clustering and genetic algorithms. *Future Internet*, 17(3):97, 2025. https://doi.org/10.3390/fi17030097.

[49] Greg Hamerly and Charles Elkan. Learning the k in k-means. In S. Thrun, L. Saul, and B. Schölkopf, editors, *Advances in Neural Information Processing Systems*, volume 16, pages 281–288. MIT Press, 2003. URL https://proceedings.neurips.cc/paper_files/paper/2003/file/234833147b97bb6aed53a8f4f1c7a7d8-Paper.pdf. Accessed: 04-21-2025.

[50] Duc Truong Pham, Stefan S Dimov, and Chi D Nguyen. Selection of k in k-means clustering. *Proceedings of the Institution of Mechanical Engineers, Part C: Journal of Mechanical Engineering Science*, 219(1): 103–119, 2005. https://doi.org/10.1243/095440605X8298.

[51] Canhong Lin, King Lun Choy, George TS Ho, Sai Ho Chung, and HY Lam. Survey of green vehicle routing problem: past and future trends. *Expert systems with applications*, 41(4):1118–1138, 2014. https://doi.org/10.1016/j.eswa.2013.07.107.

[52] Mohammed Bazirha. A novel milp formulation and an efficient heuristic for the vehicle routing problem with lunch break. *Annals of Operations Research*, 351(1): 253–278, 2025. https://doi.org/10.1007/s10479-023-05742-3.

[53] Weixuan Shi, Nengmin Wang, Li Zhou, and Zhengwen He. The bi-objective mixed-fleet vehicle routing problem under decentralized collaboration and time-of-use prices. *Expert Systems with Applications*, 273:126875, 2025. https://doi.org/10.1016/j.eswa.2025.126875.

[54] Yaling Li, Wenzhu Liao, and Yuqi Huang. Mixed fleet-based two-echelon vehicle routing optimization for cold chain logistics with diverse recharging strategies. *Plos one*, 20(2):e0318765, 2025. https://doi.org/10.1371/journal.pone.0318765.

[55] Maurizio Bruglieri, Bülent Çatay, Merve Keskin, Simona Mancini, and Ornella Pisacane. The mixed-fleet vehicle routing problem with low emission zones. *Transportation Research Part E: Logistics and Transportation Review*, 201:104230, 2025. https://doi.org/10.1016/j.tre.2025.104230.

**Contribution of Individual Authors to the Creation of a Scientific Article (Ghostwriting Policy)**

Netiphan Amphaiphan: Conceptualization, Software, Methodology, Formal analysis, Writing original draft.

Dario Landa-Silva: Conceptualization, Methodology, Writing - Review and Editing, Supervision.

Wasakorn Laesanklang: Conceptualization, Methodology, Validation, Writing - Review and Editing, Supervision, Project administration.

**Sources of Funding for Research Presented in a Scientific Article or Scientific Article Itself**

This research was partially supported by SAST Scholarship, Thailand.

**Conflicts of Interest**

The authors declare no conflict of interest.

**Creative Commons Attribution License 4.0**

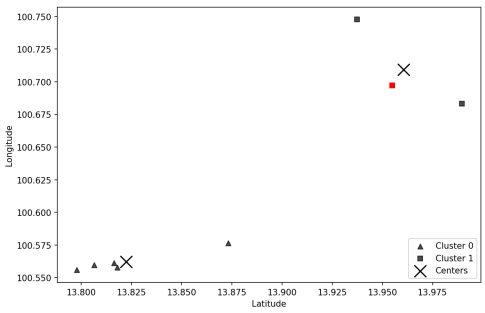
This article is published under the terms of the Creative Commons Attribution License 4.0. https://creativecommons.org/licenses/by/4.0/deed.en_US

# APPENDIX

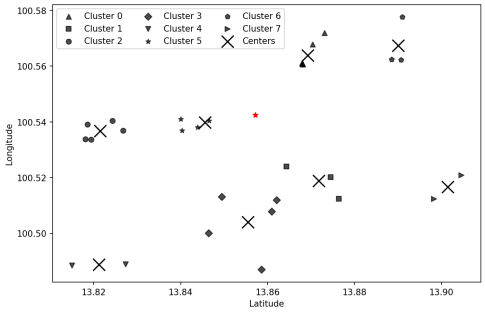
Table 1. Definitions of the sets, parameters, and variables used in the mathematical programming model.

| | |
|---|---|
| **Sets** | |
| $0, n+1$ | Vertices of the depot |
| $V$ | Set of customers |
| $V_{0,n+1}$ | Set $V$ including vertices of the depot |
| $F$ | Sets of charging stations |
| $V'$ | Set of nodes, including customers and charging stations ($V' = V \cup F$) |
| $V'_{0,n+1}$ | Set $V'$ and vertices of the depot |
| $T$ | Set of different charging technologies |
| $M_{EV}$ | Set of EVs |
| $M_{IC}$ | Set of ICVs |
| $M'$ | Set of all vehicles ($M' = M_{EV} \cup M_{IC}$) |
| **Parameters** | |
| $d_{ij}$ | Distance between vertices $i$ and $j$ |
| $t_{ij}$ | Travel time between vertices $i$ and $j$ |
| $q_i$ | Demand of vertex $i$ |
| $s_i$ | Service time of vertex $i$ ($s_0 = 0$) |
| $Q^E, Q^{IC}$ | Capacity of EVs and ICVs, respectively |
| $B$ | Battery capacity (kWh) |
| $e_i, l_i$ | Earliest and latest arrival time at vertex $i$, respectively |
| $E, L$ | Earliest and latest lunch break time, respectively |
| $D$ | Lunch break duration |
| $g_t$ | Charging rate of technology $t \in T$ (kW) |
| $cost^E, cost^{IC}$ | Travel costs per unit distance associated with EVs and ICVs, respectively |
| $c^t$ | Charging cost of technology $t \in T$ |
| $h$ | Constant energy consumption rate |
| $M$ | A big number |
| **Variables** | |
| $x^E_{ijk}$ | 1 if an EV $k$ travels from vertex $i$ to $j$, 0 otherwise |
| $x^{IC}_{ijk}$ | 1 if an ICV $k$ travels from vertex $i$ to $j$, 0 otherwise |
| $y_{ik}$ | 1 if vehicle $k$ breaks at vertex $i$, 0 otherwise |
| $W_{ik}$ | Time in which vehicle $k \in M_{EV}$ spends at vertex $i \in F$ |
| $\tau_{ik}$ | Arrival time of vehicle $k$ at vertex $i$ |
| $z_{itk}$ | Amount of energy recharged at vertex $i$ using technology $t$ of an EV $k$ |
| $E^a_{ik}$ | Amount of battery of an EV $k$ when arriving vertex $i$ |
| $E^l_{ik}$ | Amount of battery of an EV $k$ when leaving vertex $i$ |
| $\delta_{ik}$ | Slack time of vehicle $k \in M_{EV}$ at vertex $i \in F$ |

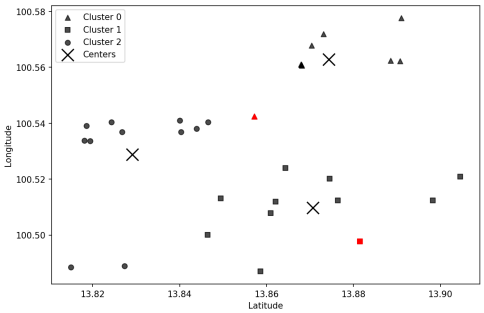
*Source: created by the authors.*



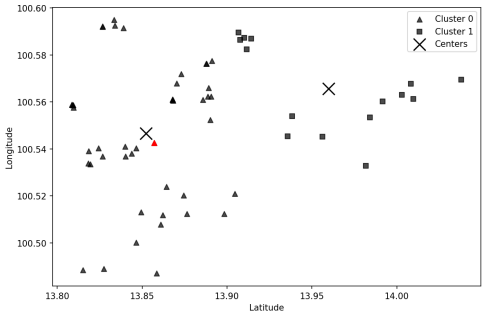

(a) clustering result for A104 with $K^* = 2$




(b) clustering result for B105 with $K^* = 8$




(c) clustering result for B205 with $K^* = 3$




(d) clustering result for C101 with $K^* = 2$

Fig. 1: Examples of results from K-means clustering. Cross markers in each subfigure represent the cluster centers and red markers indicate the location of charging stations.

*Source: created by the authors.*

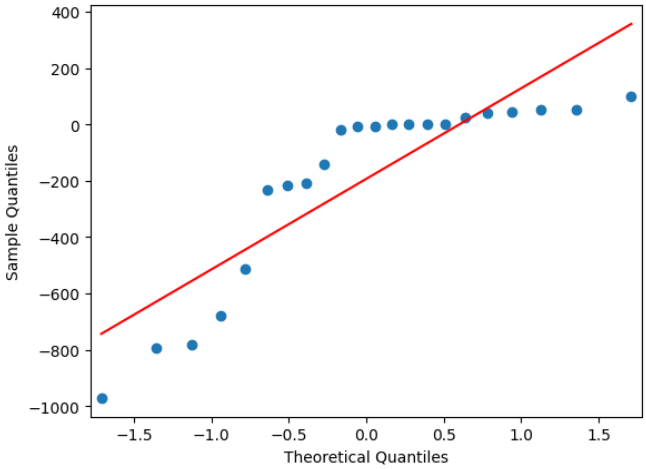



Fig. 2: Normality test for the differences of CPLEX vs Hybrid clustering using Q-Q plot

*Source: created by the authors.*

Table 5. Time (in seconds) when a solver found the first feasible solution

| Instance | w/ LB | w/o LB | Instance | w/ LB | w/o LB | Instance | w/ LB | w/o LB |
|---|---|---|---|---|---|---|---|---|
| A101 | 0.4 | 0.19 | A204 | 0.39 | 0.38 | B203 | 9.42 | 0.48 |
| A102 | 0.16 | 0.28 | A205 | 0.26 | 0.2 | B205 | 10.51 | 0.86 |
| A103 | 0.45 | 0.25 | B101 | 227 | 173 | B301 | 0.81 | 0.67 |
| A104 | 0.17 | 0.3 | B102 | 2.97 | 2.28 | B302 | 1.32 | 0.87 |
| A105 | 0.36 | 0.18 | B103 | 3.73 | 0.66 | B303 | 0.62 | 0.73 |
| A201 | 0.18 | 0.19 | B105 | 4.71 | 0.82 | B305 | 6.46 | 61.37 |
| A202 | 0.18 | 0.19 | B201 | 1.22 | 0.23 | | | |
| A203 | 0.27 | 0.41 | B202 | 2.28 | 0.67 | Avg. | 12.45 | 11.46 |

*Source: created by the authors.*

Table 6. Full report on the costs for Group A instances

| Instance | with LB | | | | | | without LB | | | | | |
|---|---|---|---|---|---|---|---|---|---|---|---|---|
| | obj. | dist. | #stops | #EVs | #ICVs | %gap | obj. | dist. | #stops | #EVs | #ICVs | %gap |
| A101 | 561.5302* | 30.7651 | 0 | 3 | 0 | 0 | 561.5302** | 30.7651 | 0 | 3 | 0 | 0 |
| A102 | 626.6316* | 63.3158 | 0 | 4 | 0 | 0 | 626.6316* | 63.3158 | 0 | 4 | 0 | 0 |
| A103 | 784.3920 | 67.1960 | 0 | 3 | 0 | 17.46 | 784.3920 | 67.1960 | 0 | 3 | 0 | 16.89 |
| A104 | 631.6537** | 64.9784 | 1 | 2 | 0 | 0 | 631.6537* | 64.9784 | 0 | 2 | 0 | 0 |
| A105 | 712.9878 | 56.4939 | 0 | 3 | 0 | 24.67 | 712.9878 | 56.4939 | 0 | 3 | 0 | 24.13 |
| A201 | 561.5302* | 30.7651 | 0 | 3 | 0 | 0 | 561.5302** | 30.7651 | 0 | 3 | 0 | 0 |
| A202 | 626.6316* | 63.3158 | 0 | 4 | 0 | 0 | 626.6316** | 63.3158 | 0 | 4 | 0 | 0 |
| A203 | 784.3920 | 67.1960 | 0 | 3 | 0 | 19.10 | 784.3920 | 67.1960 | 0 | 3 | 0 | 6.96 |
| A204 | 631.6537** | 64.9784 | 0 | 2 | 0 | 0 | 631.6537** | 64.9784 | 0 | 2 | 0 | 0 |
| A205 | 712.9878 | 56.4939 | 0 | 3 | 0 | 21.86 | 712.9878 | 56.4939 | 0 | 3 | 0 | 26.36 |
| Avg. | 748.6899 | 58.8038 | 0 | 3 | 0 | 21.86 | 748.6899 | 58.8038 | 0 | 3 | 0 | 18.59 |

Note: obj.:objective value, dist.:total distance

**integer optimal, tolerance

*Source: created by the authors.*

Table 7. Full report on the costs for Group B instances.

| Instance | with LB | | | | | | without LB | | | | | |
|---|---|---|---|---|---|---|---|---|---|---|---|---|
| | obj. | dist. | #stops | #EVs | #ICVs | %gap | obj. | dist. | #stops | #EVs | #ICVs | %gap |
| B101 | 1673.1874 | 186.5937 | 0 | 2 | 3 | 13.95 | 1673.1874 | 186.5937 | 0 | 2 | 3 | 10.75 |
| B102 | 2224.5310 | 262.2655 | 0 | 6 | 1 | 42.28 | 2075.6118 | 212.8059 | 0 | 6 | 1 | 38.67 |
| B103 | 1309.3878 | 104.6939 | 0 | 3 | 0 | 16.56 | 1515.5316 | 107.7658 | 0 | 2 | 1 | 27.97 |
| B104 | | | no sol* | | | | | | no sol* | | | |
| B105 | 1962.2140 | 106.1070 | 0 | 5 | 0 | 19.97 | 1953.945 | 101.9725 | 0 | 5 | 0 | 19.60 |
| B201 | 1625.7179 | 187.1134 | 1 | 3 | 2 | 16.12 | 1673.1878 | 186.5939 | 0 | 2 | 3 | 11.47 |
| B202 | 2264.8802 | 207.4401 | 0 | 4 | 3 | 30.58 | 2299.0048 | 199.5024 | 0 | 4 | 3 | 33.21 |
| B203 | 1369.3029 | 106.4380 | 1 | 3 | 0 | 20.09 | 1563.749 | 106.8745 | 0 | 2 | 1 | 30.18 |
| B204 | | | no sol* | | | | | | no sol* | | | |
| B205 | 1958.6774 | 104.3387 | 0 | 5 | 0 | 19.87 | 1951.8378 | 100.9189 | 0 | 5 | 0 | 19.50 |
| B301 | 1625.7179 | 187.1134 | 1 | 3 | 2 | 28.29 | 1673.1878 | 186.5939 | 0 | 2 | 3 | 23.26 |
| B302 | 2381.7674 | 237.4937 | 1 | 4 | 3 | 36.16 | 2323.1016 | 236.5508 | 0 | 4 | 3 | 35.07 |
| B303 | 1308.4606 | 104.2303 | 0 | 3 | 0 | 16.42 | 1560.4362 | 130.2181 | 0 | 3 | 1 | 30.00 |
| B304 | | | no sol* | | | | | | no sol* | | | |
| B305 | 1952.8124 | 101.4062 | 0 | 5 | 0 | 19.61 | 1961.2306 | 105.1671 | 0 | 5 | 0 | 19.96 |
| Avg. | 1804.7214 | 157.9362 | 1 | 4 | 2 | 23.33 | 1852.0000 | 155.1671 | 0 | 4 | 2 | 24.97 |

* No solution even though the computational time is increased to 180 minutes.

*Source: created by the authors.*

Table 8. Results after applying K-means

| Instance | No. clust. | avg. nodes/clus. | obj. | dist. | CT (min) | CC | #EVs | #ICVs | Time (sec) |
|---|---|---|---|---|---|---|---|---|---|
| A101 | 2 | 3.5 | 568.0892 | 34.0446 | 0 | 0 | 3 | 0 | 2 |
| A102 | 2 | 3 | 626.6276 | 63.3138 | 0 | 0 | 4 | 1 | 2 |
| A103 | 7 | 1.4 | 1567.3109 | 133.6553 | 0 | 0 | 3 | 4 | 2 |
| A104 | 2 | 3.5 | 631.6498 | 64.9767 | 1.3049 | 0.3914 | 2 | 0 | 2 |
| A105 | 6 | 1.5 | 1393.7131 | 121.8561 | 0 | 0 | 3 | 3 | 5 |
| A201 | 2 | 3.5 | 568.0892 | 34.0446 | 0 | 0 | 3 | 0 | 2 |
| A202 | 2 | 3 | 626.6276 | 63.3138 | 0 | 0 | 4 | 1 | 2 |
| A203 | 5 | 2 | 1295.8121 | 97.9059 | 0 | 0 | 4 | 1 | 5 |
| A204 | 2 | 3.5 | 631.6498 | 64.9767 | 1.3049 | 0.3914 | 2 | 0 | 2 |
| A205 | 7 | 1.4 | 1507.5984 | 203.7992 | 0 | 0 | 3 | 4 | 2 |
| B101 | 2 | 6 | 1573.6121 | 209.4907 | 3.5621 | 1.0686 | 3 | 2 | 1 |
| B102 | 2 | 10 | 2224.531 | 262.2655 | 0 | 0 | 6 | 1 | 900 |
| B103 | 2 | 9.5 | 1540.0381 | 118.2907 | 2.6587 | 0.7976 | 2 | 0 | 900 |
| B104 | 2 | 25 | 3869.3782 | 209.6891 | 0 | 0 | 5 | 3 | 900 |
| B105 | 8 | 3.75 | 2933.4024 | 142.072 | 0 | 0 | 5 | 3 | 67 |
| B201 | 2 | 6 | 1573.6121 | 209.4907 | 3.5621 | 1.0686 | 3 | 2 | 1 |
| B202 | 2 | 10 | 2224.531 | 262.2655 | 0 | 0 | 6 | 1 | 900 |
| B203 | 2 | 9.5 | 1510.351 | 105.1755 | 0 | 0 | 2 | 1 | 900 |
| B204 | 2 | 25 | 3799.9058 | 199.9529 | 0 | 0 | 5 | 3 | 900 |
| B205 | 3 | 10 | 2168.8588 | 109.4294 | 0 | 0 | 5 | 1 | 900 |
| B301 | 2 | 6 | 1573.6121 | 209.4907 | 3.5621 | 1.0686 | 3 | 2 | 1 |
| B302 | 2 | 10 | 2401.6261 | 200.3721 | 0.6783 | 0.2035 | 3 | 4 | 900 |
| B303 | 2 | 9.5 | 1283.4768 | 88.4122 | 5.1173 | 1.5352 | 2 | 0 | 900 |
| B304 | 2 | 25 | 4023.8216 | 239.9108 | 0 | 0 | 5 | 3 | 900 |
| B305 | 3 | 10 | 2168.8516 | 109.4249 | 0 | 0 | 5 | 1 | 900 |
| C101 | 2 | 30 | 4861.0776 | 255.2155 | 0.3065 | 0.3402 | 5 | 4 | 900 |
| C102 | 2 | 27.5 | 4526.914 | 238.1861 | 0.2568 | 0.2850 | 5 | 4 | 900 |
| C103 | 3 | 25 | 9280.4783 | 689.1892 | 0 | 0 | 3 | 10 | 900 |
| C201 | 2 | 30 | 5009.3884 | 229.694 | 0 | 0 | 5 | 5 | 900 |
| C202 | 2 | 27.5 | 4526.914 | 238.1861 | 0.2568 | 0.2850 | 5 | 4 | 900 |
| C203 | 3 | 25 | 9280.4783 | 689.1892 | 0 | 0 | 3 | 10 | 900 |
| C301 | 2 | 30 | 4921.2665 | 260.0592 | 0.5441 | 0.6040 | 5 | 4 | 900 |
| C302 | 2 | 27.5 | 4540.1858 | 270.0929 | 0 | 0 | 5 | 4 | 900 |
| C303 | 3 | 25 | 9280.4783 | 689.1892 | 0 | 0 | 3 | 10 | 900 |

Note: obj.:objective value, dist.:total distance, CT: charging time, CC: charging costs

*Source: created by the authors.*

Table 9. SoC sensitivity analysis.

| Instance | SoC Window | Obj. (THB) | Distance (km) | #CS Stops | %gap | Cost vs. baseline | Time Limit (min) |
|---|---|---|---|---|---|---|---|
| A101 | 25%-80% (baseline) | 561.5302 | 30.7651 | 0 | 0.01 | baseline | 15 |
| A101 | 10%-90% | 561.5302 | 30.7651 | 0 | 0.00 | +0.00% | 15 |
| A101 | 0%-100% | 561.5302 | 30.7651 | 0 | 0.01 | +0.00% | 15 |
| A102 | 25%-80% (baseline) | 626.6316 | 63.3158 | 0 | 0.00 | baseline | 15 |
| A102 | 10%-90% | 626.6316 | 63.3158 | 0 | 0.00 | +0.00% | 15 |
| A102 | 0%-100% | 626.6316 | 63.3158 | 0 | 0.00 | +0.00% | 15 |
| A103 | 25%-80% (baseline) | 784.3920 | 67.1960 | 0 | 18.77 | baseline | 15 |
| A103 | 10%-90% | 784.3920 | 67.1960 | 0 | 18.04 | +0.00% | 15 |
| A103 | 0%-100% | 784.3920 | 67.1960 | 0 | 18.28 | +0.00% | 15 |
| A104 | 25%-80% (baseline) | 633.2142 | 64.9784 | 1 | 0.01 | baseline | 15 |
| A104 | 10%-90% | 578.2068 | 64.1034 | 0 | 0.01 | -8.69% | 15 |
| A104 | 0%-100% | 578.2068 | 64.1034 | 0 | 0.00 | -8.69% | 15 |
| A105 | 25%-80% (baseline) | 712.9878 | 56.4939 | 0 | 22.65 | baseline | 15 |
| A105 | 10%-90% | 712.9878 | 56.4939 | 0 | 21.50 | +0.00% | 15 |
| A105 | 0%-100% | 712.9878 | 56.4939 | 0 | 22.54 | +0.00% | 15 |
| A201 | 25%-80% (baseline) | 561.5302 | 30.7651 | 0 | 0.01 | baseline | 15 |
| A201 | 10%-90% | 561.5302 | 30.7651 | 0 | 0.01 | +0.00% | 15 |
| A201 | 0%-100% | 561.5302 | 30.7651 | 0 | 0.01 | +0.00% | 15 |
| A202 | 25%-80% (baseline) | 626.6316 | 63.3158 | 0 | 0.01 | baseline | 15 |
| A202 | 10%-90% | 626.6316 | 63.3158 | 0 | 0.00 | +0.00% | 15 |
| A202 | 0%-100% | 626.6316 | 63.3158 | 0 | 0.00 | +0.00% | 15 |
| A203 | 25%-80% (baseline) | 784.3920 | 67.1960 | 0 | 18.26 | baseline | 15 |
| A203 | 10%-90% | 784.3920 | 67.1960 | 0 | 17.47 | +0.00% | 15 |
| A203 | 0%-100% | 784.3920 | 67.1960 | 0 | 16.93 | +0.00% | 15 |
| A204 | 25%-80% (baseline) | 675.0360 | 87.5180 | 0 | 0.00 | baseline | 15 |
| A204 | 10%-90% | 578.2068 | 64.1034 | 0 | 0.01 | -14.34% | 15 |
| A204 | 0%-100% | 578.2068 | 64.1034 | 0 | 0.01 | -14.34% | 15 |
| A205 | 25%-80% (baseline) | 712.9878 | 56.4939 | 0 | 23.24 | baseline | 15 |
| A205 | 10%-90% | 712.9878 | 56.4939 | 0 | 22.64 | +0.00% | 15 |
| A205 | 0%-100% | 712.9878 | 56.4939 | 0 | 25.43 | +0.00% | 15 |
| B201 | 25%-80% (baseline) | 1673.1878 | 186.5939 | 0 | 30.27 | baseline | 60 |
| B201 | 10%-90% | 1522.4048 | 211.2024 | 0 | 25.17 | -9.01% | 60 |
| B201 | 0%-100% | 1473.1878 | 186.5939 | 0 | 20.62 | -11.95% | 60 |
| B203 | 25%-80% (baseline) | 1310.0332 | 105.0166 | 0 | 16.82 | baseline | 60 |
| B203 | 10%-90% | 1220.1372 | 85.0686 | 0 | 10.16 | -6.86% | 60 |
| B203 | 0%-100% | 1211.0268 | 80.5134 | 0 | 9.93 | -7.56% | 60 |
| B301 | 25%-80% (baseline) | 1683.0008 | 216.5004 | 0 | 32.00 | baseline | 60 |
| B301 | 10%-90% | 1522.4048 | 211.2024 | 0 | 24.46 | -9.54% | 60 |
| B301 | 0%-100% | 1473.1878 | 186.5939 | 0 | 22.22 | -12.47% | 60 |
| B302 | 25%-80% (baseline) | 2361.4944 | 230.7472 | 0 | 37.07 | baseline | 60 |
| B302 | 10%-90% | 2277.1830 | 238.5915 | 0 | 32.29 | -3.57% | 60 |
| B302 | 0%-100% | 2148.5060 | 249.2530 | 0 | 29.47 | -9.02% | 60 |

*Source: created by the authors.*